Plant Soil
https://doi.org/10.1007/s11104-026-08368-z

RESEARCH ARTICLE

Distinctive and synergistic effects of an *Ascophyllum nodosum* extract and a nitrification inhibitor on tomato growth, photosynthetic efficiency, and metabolomic profile under low nitrogen conditions

Gianmarco Del Vecchio · Hajar Salehi · Federico Ardenti · Alejandro Castro-Cegri · Andrea Fiorini · Luigi Lucini

Received: 25 October 2025 / Accepted: 2 February 2026
© The Author(s) 2026

Abstract

Background and aims Modern agriculture requires smart and sustainable fertilization approaches. A strategy to delay the nitrification losses involves the use of nitrification inhibitors. Similarly, biostimulants may enhance nutrient uptake efficiency. This study aims to evaluate the potential synergistic effects of the 3,4-DMPP nitrification inhibitor (NI) and an *Ascophyllum nodosum*-based biostimulant (ANb) in mitigating nitrogen losses while maintaining the growth and physiological performance of tomato plants under low-nitrogen conditions.

Methods Tomato (*Solanum lycopersicum* L.) plants were subjected to different levels of nitrogen regimes combined with NI and ANb applications. Physiological traits, yield, soil and leachate nitrogen dynamics were assessed. Untargeted metabolomics of leaves and roots was performed to elucidate treatment related metabolic reprogramming.

Results Under nitrogen-limited conditions, the combined application of ANb and NI reduced NO_3^- in leached water by 48% compared to NI applied alone at 14 days after the transplant. This combined treatment enhanced photosynthetic efficiency (Phi2), during both early and late development stages, increasing Phi2 values by 34.1% and 73.5%, respectively, compared to 0% N-fertilization treatment. Untargeted metabolomics pointed out distinct metabolomic reprogramming triggered by the combination of NI with ANb, with the most pronounced modulations detected in early-stage leaves, in a way related to abiotic stress resilience, defence mechanisms, and carbon–nitrogen balance. Moreover, the combination of NI and low nitrogen resulted in lower malondialdehyde (MDA) accumulation in harvested leaves.

Conclusions Our findings confirm the impact of NI in low nitrogen conditions, while outlining the complementary and positive contribution of its combination with ANb.

Keywords Seaweed-based biostimulant · Nitrogen dynamics · Metabolomics · Photosystem II efficiency · Sustainable agriculture

Abbreviations

NI	3,4-DMPP nitrification inhibitor
ANb	*Ascophyllumnodosum*-Based biostimulant
MDA	Malondialdehyde

Responsible Editor: Cleiton Breder Eller.

G. Del Vecchio · H. Salehi · A. Castro-Cegri · L. Lucini (✉)
Department for Sustainable Food Process, Università Cattolica del Sacro Cuore, Piacenza, Italy
e-mail: luigi.lucini@unicatt.it

F. Ardenti · A. Fiorini
Department for Sustainable Crop Production, Università Cattolica del Sacro Cuore, Piacenza, Italy

L. Lucini
Institute of Bioimaging and Biological Complex Systems (IBSBC), National Research Council (CNR), Milan, Italy

Published online: 13 February 2026

NUE	Nitrogen use efficiency
N	Nitrogen
C	Carbon
NO_3^-	Nitrate
N_2O	Nitrous oxide
NH_4^+	Ammonium
$N–NO_3^-$	N-nitrate
$N–NH_4^+$	N-ammonium
DAT	Days after transplanting
WHC	Water Holding Capacity
Phi2	Quantum yield of photochemical energy conversion in PSII
PhiNO	Quantum yield of non-regulator non-photochemical energy loss in PSII
PhiNPQ	Quantum yield of regulated non-photochemical energy loss in PSII
ESL	Early-stage leaf samples
LSL	Late-stage leaf samples
RS	Root samples
VIP	Variable Importance in Projection

Introduction

Nitrogen (N) is an essential element for all living organisms, and nitrogen-containing compounds are widely involved in plants in photosynthesis, carbon (C) and N metabolism, hormone regulation, and many other physiological processes (Anas et al. 2020). Still, nitrogen is often the most limiting among soil nutrients (Ågren et al. 2012), making nitrogen-based fertilizers indispensable for modern agriculture, which is required to meet the food demand of a constantly growing global population (Stewart et al. 2005). However, their massive application has altered the nitrogen cycle, negatively impacting human health, biodiversity, and crop yields (Howarth 2004).

One explanation is given by plants' inefficient nitrogen use efficiency (NUE), measuring the system's efficiency in converting nitrogen inputs into yield outputs (Fageria and Baligar 2005). Notably, data has demonstrated that more than half of the nitrogen applied as fertilizer is lost to the environment through gaseous and hydrological pathways (Lassaletta et al. 2014). Motavalli et al. (2008) pointed out that nitrogen losses in agriculture primarily occur as nitrate leaching, erosion, and runoff in the soil and as ammonia and nitrogen oxides in the atmosphere. Specifically, elevated nitrate levels in groundwater pose serious human health risks (Ward et al. 2018) and harm aquatic biodiversity (Banerjee et al. 2023). Consequently, several solutions have been investigated to mitigate nitrogen losses and reduce synthetic fertilizer usage in modern agriculture. These efforts aim to promote greener, more sustainable, and regenerative agricultural practices (Mahmud et al. 2021). Significant attention has been paid to nitrification inhibitors among the emerging alternative nutrient management strategies. These molecules can reduce nitrogen losses in the forms of nitrate (NO_3^-) and nitrous oxide (N_2O), thereby improving nitrogen use efficiency (NUE) and enhancing nitrogen uptake by the rhizosphere (Beeckman et al. 2024; Qiao et al. 2015; Abalos et al. 2014). One of the most widely used is 3,4-dimethylpyrazole phosphate (3,4-DMPP, referred to as NI in the text). 3,4-DMPP has been investigated to reduce nitrogen losses and enhance nitrogen uptake efficiency significantly (Li et al. 2008; Menéndez et al. 2012; Martínez-Alcántara et al. 2013). Specifically, it delays the oxidation of ammonium (NH_4^+) by inhibiting the enzymatic activity of nitrifying bacteria, particularly *Nitrosomonas*, in the initial stage of the nitrification process. This inhibition typically lasts from 4 to 10 weeks under field conditions, depending on temperature, and results in reduced nitrate (NO_3^-) leaching and nitrous oxide (N_2O) emissions (Vilas et al. 2019; Zerulla et al. 2001). Indirectly, its application enhances nitrogen utilization efficiency, potentially leading to reduced nitrogen fertilizer applications.

On the other hand, another alternative to mitigating the severe environmental threats posed by synthetic fertilizers is given by plant biostimulants. According to Du Jardin (2015), biostimulants are substances or microorganisms that enhance plant tolerance to abiotic stress, improve crop quality traits, and increase nutrient efficiency. This effectiveness is achieved by improving nutrient uptake by roots and minimizing nutrient losses (Li et al. 2022; Calvo et al. 2014). A broad class of substances classified as biostimulants include seaweed extracts, which have been found to positively impact plant growth and yield (Kumar et al. 2024; Craigie 2011). Notably, several commercial formulas based on *Ascophyllum nodosum* (ANb), a brown rockweed found on the Atlantic coasts of northern Europe and North America, have been proven as able to promote plant growth (Shukla et al. 2019) and to enhance nitrogen use efficiency (NUE)

by improving nitrogen uptake and nitrate utilization (Goñi et al. 2021). This highlights the potential environmental benefits of ANb extracts as an alternative to extensive synthetic nitrogen fertilizer use.

The pressing need to reduce fertilizer application calls for scientists to uncover innovative solutions that ensure optimal plant growth and yield while minimizing nitrogen losses. One potential approach may involve the combined application of ANb and 3,4-DMPP. However, while the individual effects of NI in reducing nitrification activity and of ANb in enhancing nitrogen uptake have been relatively well investigated, their combined application remains poorly explored, and its potential benefits for plant performance and nitrogen management are not yet understood. On this basis, investigating the combined strategy involving NI and ANb may provide valuable insight into whether their complementary actions can contribute to improving nitrogen dynamics within the plant-soil system.

The goal of this study is to explore the effect of NI (3,4-DMPP, marketed as Vibelsol®), alone or combined with an *Ascophyllum nodosum* extract (Elitesea, ACADIAN) under low nitrogen conditions, focusing on tomato (*Solanum lycopersicum* L.*)* as a model crop. Particularly, the study focused on low nitrogen availability, as this condition may represent a relevant context for evaluating potential synergistic interactions between NI and ANb, an aspect that can be masked under optimal nitrogen supply. More specifically, one objective is to assess whether the application of NI and its combination with ANb might improve agronomic and photosynthetic performance while reducing nitrogen losses, particularly under heavy rainfall. Additionally, the research examines metabolomic modulations by analysing the impact of NI alone and in combination with ANb in leaves collected at different growth stages and in roots.

Material and methods

Plant materials and growth conditions

Tomato seeds (*Solanum lycopersicum* L., cultivar N507F1 by Nunhems, Sant'Agata Bolognese, Italy) were sown in polystyrene boxes filled with peat substrate. Seedlings were transplanted into pots (40 cm × 16 cm) 20 days after sowing. Two different substrates were used to fill pots: a 5 cm layer of perlite was placed at the bottom, topped with 30 cm of sandy loam soil (7.2% sand, 24.0% silt, and 68.8% clay). The specific characteristics of the sandy loam soil included a 6.5 pH in water, an electrical conductivity of 379 µs/cm, 1.1 g/kg of total Kjeldahl nitrogen, and 16.7 g/kg of organic matter. After transplanting, tomato plants were grown for 85 days, from 14th June 2023 to 7th September 2023, under semi-controlled conditions, in an upper-closed chamber designed to shield from rainfall and maintain outdoor temperatures. The experiment was run at the experimental station of Università Cattolica del Sacro Cuore (45.036110 N; 9.726810E) located in Piacenza (Italy). The average daily temperatures from transplanting to harvesting ranged from 20.7 to 31.3 °C, representing the maximum and minimum limits, respectively. Peak temperatures were recorded on the 23rd, 24th, and 25th of August, reaching highs of 38.1, 38.4, and 38.5 °C, respectively. The average, minimum, and maximum temperature of the experimental period are reported in Figure S1.

Experimental treatments and biostimulant application

Six different treatments, each with four biological replicates, were applied as follows: (1) 0% N-fertilization; (2) 100% N-fertilization (Belprime 38S); (3) 60% N-fertilization (Belprime 38S); (4) 100% N-fertilization and NI (RT 38S); (5) 60% N-fertilization and NI (RT 38S); (6) 60% N-fertilization and NI (RT 38S) with four applications of ANb. The 100% fertilization dosage corresponded to 100 kg N ha^{-1}. The 60% N fertilization rate was selected as a low-N supply to represent a substantial reduction relative to the full fertilization rate recommended on the fertilizer label, while avoiding extreme N deprivation that could lead to masking treatment-specific responses. Belprime 38S and RT 38S, both sourced from Belor Toscana s.r.l. (Fucecchio, Florence, Italy) have the same chemical composition: 6.5% ammoniacal nitrogen, 31.5% urea nitrogen, and 18% soluble sulfur trioxide. However, RT 38S is additionally enriched with the addition of NI.

The *Ascophyllum nodosum*-based biostimulant Elitesea (ANb) supplied by ACADIAN (Dartmouth, Nova Scotia, Canada) was used according to label recommendations. In detail, Elitesea was applied four times by drench application at 21-day intervals

to 60% N-fertilizer treatments with NI, starting from transplant. ANb extracts were prepared at a 0.35% concentration, and the application volume was adjusted to 80% of the soil's Water Holding Capacity (WHC).

Agronomic assessments

Tomato yield was quantified by measuring each plant's fresh mass of ripe fruits. Sampling was conducted when more than 95% of the fruits were fully ripened. Aboveground vegetative biomass was measured as the dry mass of the remaining plant parts, excluding fruits. A 100 g subsample was taken from each biomass sample to determine dry matter content by oven-drying at 65 °C until a constant weight was achieved. The nitrogen concentration in fruits and vegetative biomass was determined using the Kjeldahl method. Nitrogen uptake was calculated by multiplying the fresh tomato yield and the dry mass of the vegetative biomass by their respective nitrogen concentrations.

Soil sampling was performed 14 and 27 days after transplanting (DAT) to assess soil N-ammonium ($N–NH_4^+$) and N-nitrate ($N–NO_3^-$) concentrations. These two time points were selected to capture the early stage of crop development, during which the inhibitory activity of NI (3,4-DMPP) has been reported to be most pronounced, typically persisting for several weeks following application under moderate to warm seasonal temperature conditions (Vilas et al. 2019; Zerulla et al. 2001) Soil $N\text{-}NO_3^-$ and $N\text{-}NH_4^+$ concentrations were analyzed on 5 g of homogeneously mixed soil extracted with 20 mL of potassium sulphate (K_2SO_4, 0.5 M) and pipetted into 96-well quartz microplates. $N\text{-}NO_3^-$ and $N\text{-}NH_4^+$ were assessed with dual-wavelength UV spectroscopy (275, 220 nm) on acidified (HCl 1 M) samples. Heavy rain simulation to assess nitrogen leaching trails was performed 14 and 27 days after transplanting, immediately after soil sampling, by applying an equal volume of water to each pot across all treatments, corresponding to 200% of WHC. After 24 h, the leached water was collected from underpots. Leached $N\text{-}NO_3^-$ concentrations were assessed using the same spectroscopy method described for soil samples.

Photosynthetic performance

Four different photosynthetic measurements were conducted on tomato leaves using the MultisepQ 2.0 device (PhotosynQ, East Lansing, MI, USA), with each analysis performed under comparable irradiance conditions at intervals of eight to fourteen days after each of the four biostimulant applications, to ensure representation of major growth stages and ANb-driven physiological effects. Analyses were conducted at 13, 35, 56 and 71 DAT, referred to as T1, T2, T3, and T4, respectively, in the results and discussion sections. The parameters under investigation were the quantum yield of photochemical energy conversion in PSII (Phi2), the quantum yield of non-regulator non-photochemical energy loss in PSII (PhiNO), and the quantum yield of regulated non-photochemical energy loss in PSII (PhiNPQ) (M.Kramer et al. 2004).

Untargeted metabolomics analysis for leaves and roots

Two samplings for leaves and one for roots were collected from each biological replicate to run untargeted metabolomics using ultra-high performance liquid chromatography coupled to quadrupole time-of-flight mass spectrometry. The first set of early-stage leaf samples (ESL) were collected at 47 DAT, while the second set of late-stage leaf samples (LSL) was collected at 85 DAT by sampling leaves from the first to the third branch starting from the shoot apex. Root samples (RS) were collected 85 DAT from secondary and tertiary root parts only after washing the entire root system from soil residues using tap water and a sieve. Afterwards, root and leaf samples were homogenized in liquid nitrogen with a pestle and mortar. Metabolites were extracted by blender homogenization (Polytron PT 1200 E, Kinematica AG, Switzerland) from 1.00 g of leaf and root in 10 mL of 80% methanol and 0.1% formic acid (both from Sigma-Aldrich, St. Louis, MO, USA). Extracts were then centrifuged (10,000 × g, 15 min) and filtered (0.22 µm cellulose membrane) into vials. The metabolomic analysis was carried out using ultra-high-pressure liquid chromatography coupled with quadrupole-time-of-flight mass spectrometry (1290 UHPLC and 6550 iFunnel QTOF-MS from Agilent Technologies, Santa Clara, CA, USA) as previously

described by Salehi et al. (2023). A volume of 3 µL for leaf and 6 µL for root samples was injected and a reverse-phase chromatography method with a gradient elution of water and acetonitrile was used for separation. The acetonitrile concentration increased from 6 to 94% in 33 min, with a flow set at 0.2 mL/min. The column used for the separation phase was an Agilent Plus C18 analytical column with 1.7 µm particle size, and the mass spectrometer acquisition was made in SCAN across a range of 100–1200 m/z with positive polarity and with a resolution of 30,000 full width at half maximum (FWHM). Annotation of raw data was performed by using Profinder B10.0 (Agilent Technologies, Santa Clara, CA, USA), applying the "find-by-formula" algorithm (monoisotopic mass, isotope spacing and ratio) against PlantCyc database 9.6 (Hawkins et al. 2021), achieving a level 2 of annotation, as referred to COSMOS standards in metabolomics (Salek et al. 2013). QC samples were prepared by pooling equal aliquots from all individual samples and randomly injected throughout the sequence. QC samples were analysed using data-dependent MS/MS fragmentation (N = 9 top ions) with collision energies of 10, 20, and 40 eV (Salehi et al. 2023).

MDA assay

The lipid peroxidation level was quantified as malondialdehyde (MDA) content by performing the TBARS assay (Heath and Packer 1968) in leaves at harvest with minor modifications (Carvajal et al. 2017). For each plant, 100 mg of fresh leaves were collected and processed by using a mixture of 1.5 mL of 20% trichloroacetic acid (TCA) and 0.3 mL of 4% butylated hydroxytoluene (BHT). The homogenates were subjected to two centrifugation steps (10 min, 10,000 × *g*, 4 °C), and 0.25 mL of supernatant was then mixed with 0.75 mL of 0.5% thiobarbituric acid (TBA) and subsequently heated for 30 min at 94 °C, followed by 10 10-min cooling period on ice to stop the reaction. Three replicates were prepared for each sample, and absorbance was measured at 532 nm and 600 nm. Results were determined using a standard curve and presented as µg of MDA per kg of fresh weight.

Statistical analysis

One-way ANOVA followed by Duncan post-hoc test ($p < 0.05$) was performed to analyze agronomic, photosynthetic, and MDA assays. Metabolomics data were elaborated in Mass Profiler Professional B15.1 (Agilent Technologies) (Benjamin et al. 2019), and compounds' abundance was log2-transformed, normalized to the 75th percentile, and then baselined against the median in the dataset. To naively evaluate patterns among treatments, hierarchical cluster analysis (HCA – Euclidean distance, Ward's linkage) was initially performed based on a fold-change (FC) heat map. Datasets were then imported into SIMCA 17 (Umetrics, Malmo; Sweden) for supervised multivariate modelling using orthogonal projection to latent structures discriminant analysis (OPLS-DA). The resulting models were cross-validated (CV-ANOVA; $p < 0.05$), and then outlier detection (Hotelling's T2) and goodness parameters (R^2Y goodness-of-fit, and Q^2Y goodness-of-prediction) were evaluated. To exclude model overfitting, permutation tests were performed (n = 100). Afterwards, Variable Importance in Projection (VIP) analysis identified metabolites with the highest discriminant potential score (VIP > 1.1). Thereafter, Volcano plot analysis ($p < 0.05$; Fold Change > 1.0) was run to identify statistically differential metabolites and pathway analysis by the Omics Viewer Pathway Tool in PlantCyc (Stanford, CA, USA) was used for interpretations (Caspi et al. 2013). Venn analysis on ESL was run selecting metabolites that met two criteria: (1) a Variable Importance in Projection (VIP) score higher than 1.0, identified via pairwise OPLS-DA comparisons between the control and the treatments, and (2) statistical significance determined by Volcano analysis.

Results

Agronomic parameters and lipid peroxidation levels

Tomato yield and plant biomass were significantly affected by the nitrogen fertilization treatments (Table 1). The control and 60% N-fertilization treatments exhibited significantly lower fresh yields than other N-fertilization treatments. Specifically, the control treatment resulted in the lowest fresh yield (245 g), while the 60% N-fertilization combined with ANb and NI produced the highest yield (628 g). However, no statistically significant differences were observed between the latter and the 100%

Table 1 Tomato yield (g), above-ground biomass, nitrogen uptake of fruits, N-uptake of biomass, and malondialdehyde (MDA) content in leaves across treatments

	Yield (g)	Above Ground Biomass (g)	N-Uptake Fruit (g)	N-Uptake Biomass (g)	MDA(μg g^{-1} FW)
Control	245 ± 19 **b**	35.8 ± 7.2 **b**	0.31 ± 0.03 **b**	0.35 ± 0.07 **d**	15.63 ± 2.60 **b**
100% N-fert	571 ± 115 **a**	58.1 ± 6 **a**	1.04 ± 0.25 **a**	0.99 ± 0.06 **a**	14.42 ± 1.34 **ab**
60% N-fert	337 ± 32 **b**	30.2 ± 2.4 **b**	0.43 ± 0.03 **b**	0.39 ± 0.07 cd	15.56 ± 1.22 **b**
100% N-fert—NI	577 ± 94 **a**	49.1 ± 13.3 **ab**	0.95 ± 0.02 **a**	0.79 ± 0.19 **ab**	15.48 ± 3.75 **b**
60% N-fert—NI	624 ± 101 **a**	41.6 ± 9.2 **ab**	1.06 ± 0.14 **a**	0.60 ± 0.07 **bcd**	12.38 ± 2.04 **a**
60% N-fert—NI—ANb	628 ± 60 **a**	46.4 ± 10 **ab**	1.03 ± 0.27 **a**	0.63 ± 0.08 **bc**	12.64 ± 2.73 **a**
Significance	***	**	***	***	*

N-fertilization treatments (with or without NI) or the 60% N-fertilization treatment with NI (Table 1).

Aboveground vegetative biomass production was highest under 100% N-fertilization (58.1 g) and was significantly different from the control (35.8 g) and 60% N-fertilization (30.2 g) treatments. No significant differences were detected between 100% N-fertilization and 100% N-fertilization with NI, 60% N-fertilization with NI and ANb, or 60% N-fertilization with NI treatments (Table 1).

Nitrogen uptake in fruits followed a similar trend to fresh yield. The control and 60% N-fertilization treatments exhibited the lowest N uptake among all treatments. The highest N uptake in fruits (1.06 g) was recorded under the 60% N-fertilization with NI treatment. However, this was not significantly different from the 100% N-fertilization treatments or the 60% N-fertilization treatments with NI and ANb (Table 1).

Nitrogen uptake in vegetative biomass was generally increased under the 100% N-fertilization treatments (Table 1), particularly in the absence of NI (0.99 g). In contrast, the control treatment resulted in the lowest N uptake in vegetative biomass (0.35 g), which was significantly lower than that observed in the 100% N-fertilization treatments (with or without NI) and the 60% N-fertilization treatments with NI and ANb (Table 1). Interestingly, our results suggest a possible difference in N partitioning among treatments, between fruits and vegetative biomass, despite future and more targeted investigations are needed.

MDA assay, performed on leaves to evaluate lipid peroxidation, showed differences across treatments. Both 60% N-fertilization with NI treatments, regardless of ANb application, significantly reduced MDA content. Specifically, MDA content decreased by 21% in 60% N-fertilization with NI treatment and by 19% in the 60% N-fertilization with NI and ANb treatment, while the control exhibited the highest MDA levels (Table 1).

Overall, NI-treated plants showed similar yields, biomass and MDA levels, irrespective of N levels, possibly overcoming ANb effects on these parameters under limiting conditions.

Data are presented as mean ± standard deviation. Different lowercase letters indicate significant differences between treatments based on one-way ANOVA with Duncan's post hoc test, while asterisks (*) denote statistically significant differences at $p < 0.05$.

Nitrogen levels in soil and leaching water

Soil $N–NO_3^-$ and $N–NH_4^+$ concentrations were significantly affected by fertilization treatments at both 14 and 27 days after transplant. At 14 DAT, $N–NO_3^-$ concentration was generally higher under N-fertilization treatments without NI than with it. Specifically, the 100% N-fertilization treatment showed the highest value (58.8 mg kg^{-1}). Conversely, the control had the lowest $N–NO_3^-$ concentration (32.3 mg kg^{-1}), which was not statistically different from the 100% N-fertilization with NI or the 60% N-fertilization with NI and ANb. At 27 DAT, differences in $N–NO_3^-$ concentrations among treatments were less pronounced. The control exhibited a significantly lower concentration (5.6 mg kg^{-1}) than other treatments. No significant differences were observed among the other fertilization treatments, which averaged 46.2 mg kg^{-1} (Table 2).

Table 2 Soil N–NO_3^-, Soil N–NH_4^+, and leached N–NO_3^- concentrations at 14 and 27 days after transplanting (DAT)

	Soil N–NO_3^- (mg kg^{-1})		Soil N–NH_4^+ (mg kg^{-1})		Leached N–NO_3^- (mg L^{-1})	
	14 DAT	27 DAT	14 DAT	27 DAT	14 DAT	27 DAT
Control	32.3 ± 3.8 **c**	5.6 ± 0.5 **c**	12.7 ± 0.5 **c**	15.8 ± 3.1 **b**	74 ± 30.8 **b**	223 ± 22.7
100% N-fert	58.8 ± 0.4 **a**	48.3 ± 0.2 **b**	31.3 ± 6.5 **ab**	20.3 ± 2.2 **b**	242.5 ± 31.1 **a**	244 ± 44.1
60% N-fert	58.3 ± 4.3 **a**	46.3 ± 1.9 **b**	14.7 ± 1.8 **c**	14.7 ± 0.6 **b**	262 ± 4 **a**	265 ± 2.6
100% N-fert—NI	39.4 ± 11.9 **bc**	44.9 ± 1.2 **b**	39.7 ± 8.4 **a**	42 ± 13.6 **a**	230.5 ± 18.43 **a**	252 ± 8.5
60% N-fert—NI	47.9 ± 5.3 **ab**	45.6 ± 1.2 **b**	35.8 ± 9 **ab**	25.1 ± 6.2 **b**	209 ± 41.9 **a**	237 ± 58.4
60% N-fert—NI—ANb	42.3 ± 9.6 **bc**	46.1 ± 0.9 **b**	29.5 ± 6.6 **b**	24.5 ± 7.4 **b**	109.3 ± 33.5 **b**	248 ± 12.2
Significance	***	***	***	***	***	**ns**

At 14 DAT, soil N–NH_4^+ concentration was highest under 100% N-fertilization with NI (39.7 mg kg^{-1}) and generally higher in other treatments with NI, as well as in the 100% N-fertilization without NI. Conversely, soil N–NH_4^+ concentrations were lower in control (12.7 mg kg^{-1}) and in the 60% N-fertilization without NI (14.7 mg kg^{-1}). After 27 DAT, 100% N-fertilization with NI resulted in the highest soil N–NH_4^+ concentration (42.0 mg kg^{-1}), significantly greater than all other treatments. The remaining treatments showed no statistical differences and averaged 20.1 mg kg^{-1} (Table 2).

After 14 DAT, leached N–NO_3^- was significantly reduced in the control (74.0 mg L^{-1}) and in the 60% N-fertilization with NI and ANb (109.3 mg L^{-1}) compared to other treatments (Table 2). Notably, the 60% N-fertilization with NI and ANb decreased leached N–NO_3^- by 48% compared to the same fertilization level with NI alone. No statistical differences were observed in leached N–NO_3^- between the 100% N-fertilization treatments (with or without NI) and the 60% N-fertilization treatment. Moreover, no further differences were observed in N–NO_3^- analysis after 27 days after the transplant (Table 2).

Data show the mean ± standard deviation, and different lowercase letters and asterisks indicate differences between treatments after one-way ANOVA with Duncan's post hoc test and significant difference (* $p < 0.05$), respectively.

Metabolomic profile of leaves and roots

The untargeted metabolomics identified over 2000 metabolites in leaf samples at both ESL and LSL and more than 500 metabolites in RS. The whole dataset, including individual abundances, mass spectra, and retention time, is provided in Supplementary Table S1. An overview of the differences and similarities across all treatments was achieved through three hierarchical cluster analyses (HCA) based on fold change values for each dataset. In the ESL analysis, NI was the primary distinguishing factor, with treated leaves exhibiting distinct metabolic profiles compared to untreated ones. Additionally, within NI treatments, samples from ANb-treated plants formed a distinct cluster, highlighting the strong influence of the biostimulant on this matrix (Fig. 1). A similar pattern emerged in the LSL analysis, where NI remained the most influential factor, though treatment separation was less pronounced than in the ESL (Figure S2A). Coherently with LSL result, the RS analysis also showed a slight clustering of NI-treated samples, confirming NI as the dominant variable over AN application and fertilization levels (Figure S2B). However, the most significant differences in the metabolomic profiles among treatments were observed in the ESL, leading to a primary focus on this analysis.

Metabolic modulation by NI across N-fertilization levels

To better assess the impact of NI at different N fertilization levels on both leaves and roots, we compared plants receiving only N-fertilizer (100% and 60% N fertilization) with those supplemented with NI (100% and 60% N fertilization with NI).

Firstly, an OPLS discriminant multivariate analysis was performed on ESL, LSL, and RS to validate the results from unsupervised models. Despite all three models showing positive parameters ($R^2Y > 0.97$ and $Q^2Y > 0.62$ in all three models), differences among treatments were distinct. Specifically, the ESL score

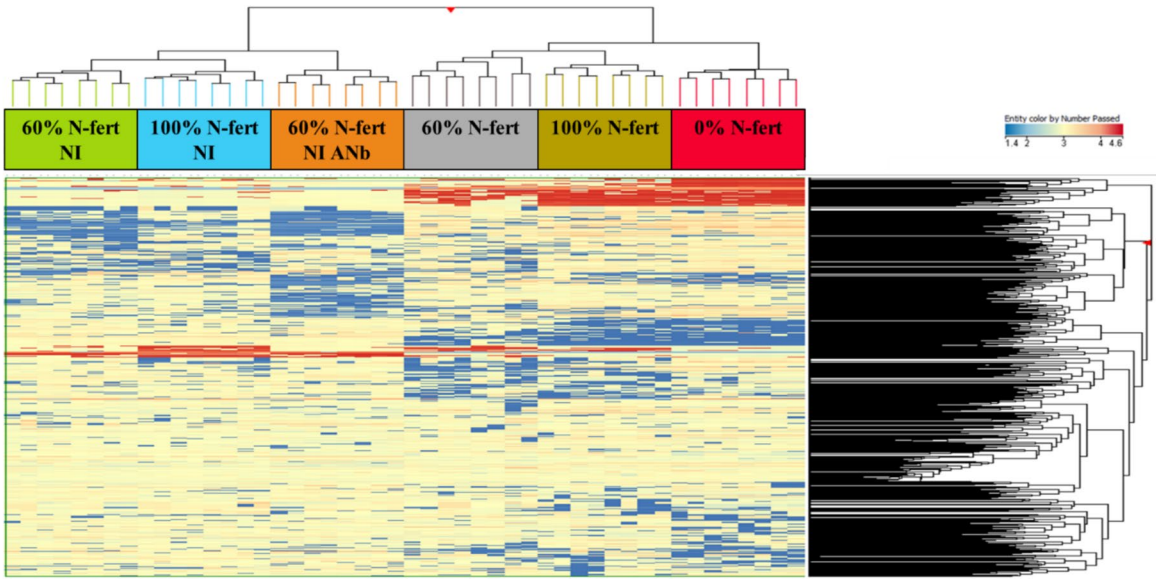

Fig. 1 Unsupervised hierarchical clustering analysis (HCA) of the metabolomic profile of ESL of tomato plants grown under control, varying N-fertilizer levels, and treatments with NI and ANb. Hierarchical clusters (linkage rule: Ward; distance matrix: Euclidean) were based on the fold-change-based heat map of compounds' normalized intensities

plot aligned with the HCA model, separating NI-treated samples from untreated ones. In contrast, the LSL model showed a less pronounced separation of NI treatments from the others, while the RS model revealed no clear separation, with overlapping samples from 100% N-fertilization and 60% N-fertilization with NI (Figure S3). The full list of statistically significant VIP markers (> 1.1) is provided in Supplementary Table S2.

A deeper comparison of metabolomic differences was achieved through PlantCyc pathway analysis. Notably, ESL exhibited the most significant modulation, with 343 metabolites affected, whereas only 92 and 123 metabolites were significantly altered in LSL and RS, respectively. In ESL, despite differing fertilisation levels, both NI treatments induced remarkably similar metabolic changes (Fig. 2A). NI application primarily affected the biosynthetic pathways of amino acids, fatty acids, and aromatic compounds. Specifically, it led to a general down accumulation of amino acid and fatty acid biosynthesis. In fatty acid metabolism, a decrease in compounds mainly associated with phospholipid and sphingolipid pathways was observed, while lipids related to cuticular wax biosynthesis were significantly accumulated. Similarly, NI treatments caused a reduction in aromatic compounds, particularly affecting cinnamate, flavonoid, and coumarins biosynthesis. However, no notable differences were observed in LSL and RS analysis, likely due to a reduced number of significant compounds in these two matrices.

Then, a Venn analysis was performed on the ESL samples, as they showed the greatest heterogeneity among various treatments, to assess the impact of NI by examining compounds shared between the 100% N-fertilization and NI and 60% N-fertilization with NI treatments. Notably, 55 compounds were exclusively shared by the NI treatments, which was six times greater than the 9 compounds regulated only by the non-NI treatments. All 55 metabolites presented consistent fold-change (FC) trends across the two NI treatments. Analysis of these metabolites revealed modulations in compounds involved in cell membrane structure and function, terpenoid and phenylpropanoid biosynthesis, and IAA inactivation (Fig. 2B). Specifically, 16-feruloyloxypalmitate and 16-sinapoyloxypalmitate, both produced by 16-hydroxypalmitate, showed high positive Log FC and were linked to the formation of aromatic domains in suberin biosynthesis, a key component of specialized plant cell walls.

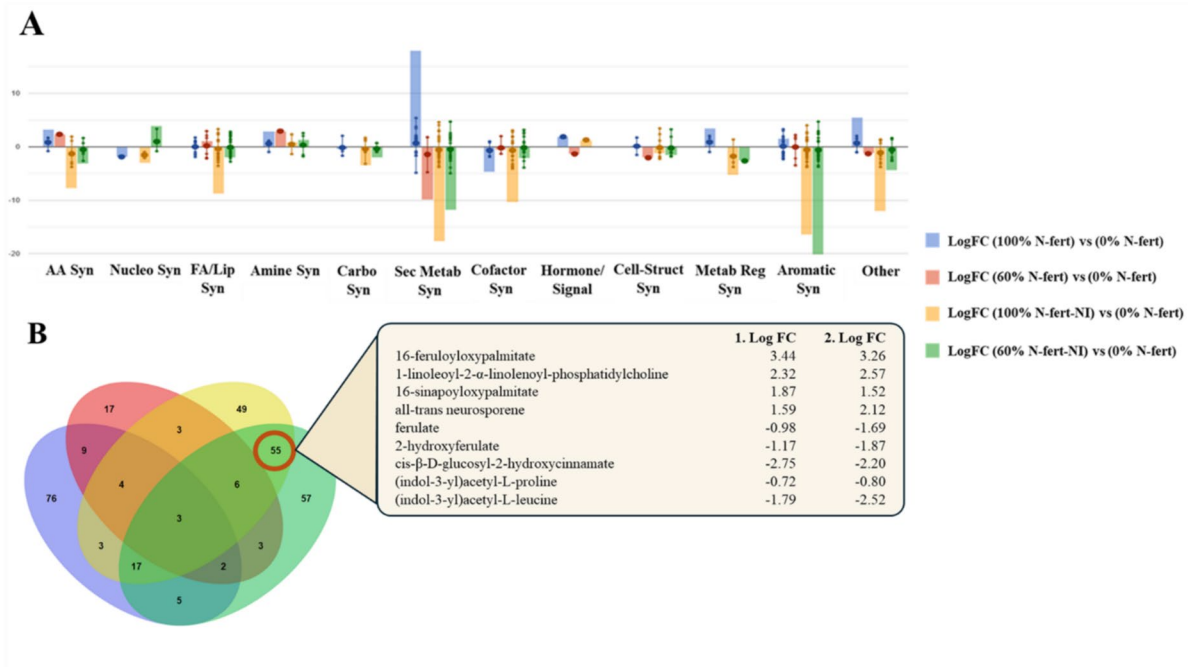

Fig. 2 Biosynthetic metabolism processes (**A**) and Venn analysis (**B**) of ESL, modulated by treatments with 100% N-fertilization, 60% N-fertilization, 100% N-fertilization with NI, and 60% N-fertilization with NI. **(A)** The metabolomic pathways were obtained using the Omics Viewer Dashboard of the PlantCyc Pathway Tool software (www.plantcyc.com). Each set of subcategories and the cumulative Log FC (sumFC) are represented on the x-axis and y-axis, respectively. Abbreviations stand for: AA = Amino Acid; Nucleo = Nucleotide; FA/Lip = Fatty acid and Lipid; Carbo = Carbohydrate; Sec Metab = Secondary Metabolite; Cell-Struct = Cell-Structure; Metab Reg = Metabolic Regulation; Syn = Biosynthesis. (**B**) Venn analysis of significative metabolites modulated among the four treatments. The box contains some metabolites shared between the two NI treatments, with their Log FC values. 1.Log FC and 2.Log FC correspond to the 100% N-fertilization with NI treatment and 60% N-fertilization with NI treatment, respectively

Positive Log FC was also observed for 1-linoleoyl-2-α-linolenoyl-phosphatidylcholine, involved in phospholipid desaturation. Similarly, all-trans neurosporene, a key intermediate in lycopene biosynthesis, followed the same positive Log FC trend and contributed to carotenoid biosynthesis. Interestingly, three compounds associated with coumarin biosynthesis -ferulate, 2-hydroxyferulate, and cis-β-D-glucosyl-2-hydroxycinnamate—were down-accumulated in NI treatments. Additionally, the biosynthesis of the hormone IAA was negatively affected, as down accumulation of (indol-3-yl)acetyl-L-proline and (indol-3-yl) acetyl-L-leucine was observed.

Metabolic reprogramming upon Aschophyllum nodosum (ANb) application

To specifically investigate the potential role of ANb application in conjunction with NI, treatments with NI (100% N-fertilization with NI, 60% N-fertilization with NI) were compared to the treatment involving both NI and ANb (60% N-fertilization with NI and ANb application).

First, an OPLS discriminant multivariate analysis was conducted on ESL, LSL, and RS, with all three models showing adequate scores ($R^2Y > 0.97$ and $Q^2Y > 0.68$ in all three models). However, only the ESL model presented a slight differentiation between the NI-treated treatments and the ANb treatment, while no significant separation was observed in the LSL and RS models (Figure S4). A full list of statistically significant VIP markers (> 1.1) is provided in Supplementary S3.

To further interpret the impact of ANb in the presence of NI, a pathway analysis was performed for ESL, LSL, and RS. The results indicated that ANb application significantly modulates secondary metabolites and lipid biosynthesis in ESL (Fig. 3A).

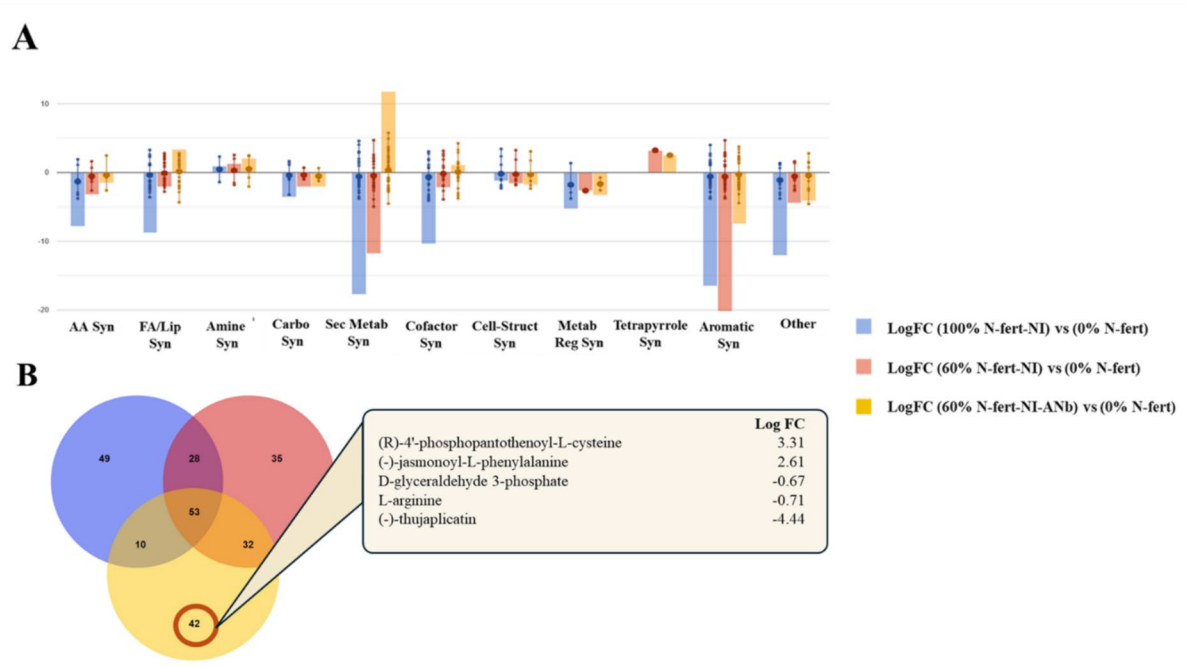

Fig. 3 Biosynthetic metabolism processes (**A**) and Venn analysis (**B**) of ESL, modulated by treatments with 100% N-fertilization with NI, 60% N-fertilization with NI, and 60% N-fertilization with NI and ANb (**A**) The metabolomic pathways were obtained using the Omics Viewer Dashboard of the PlantCyc Pathway Tool software (www.plantcyc.com). The x-axis represents metabolic subcategories, while the y-axis shows the cumulative Log FC (sumFC). Abbreviations: AA = Amino Acid; Nucleo = Nucleotide; FA/Lip = Fatty acid and Lipid; Carbo = Carbohydrate; Sec Metab = Secondary Metabolite; Cell-Struct = Cell-Structure; Metab Reg = Metabolic Regulation; Syn = Biosynthesis. (**B**) Venn analysis of significant metabolites modulated across the three treatments. The box highlights a selection of metabolites exclusively modulated by ANb + NI treatments, with their Log FC values

Secondary metabolism showed a marked accumulation of alkaloids, including betanin and lampranthin I. Among lipid biosynthesis, an increase in the accumulation of hydroxylated lipids (such as1-palmitoyl-2-vernoloyl-phosphatidylcholine), and long-fatty acid activation pathway (such as 9(10)-EpODE, (13S)-HPODE and di-homo-γ-linolenate) was observed exclusively in the ANb treatment (Fig. 3A). A distinct metabolic reprogramming was observed in LSL and RS, where differences were almost flattened along treatments.

Moreover, further analysis was conducted to identify metabolites significantly differentiating the *Aschopyllum nodosum*-treated plants in ESL. A Venn diagram analysis was performed to identify compounds modulated across the three treatments. Of the compounds analysed, 21.28% were common to all treatments, while 16.87% were exclusive to the treatment with ANb application. Notably, the 60% N-fertilization with NI and ANb treatment showed an accumulation of metabolites involved in various metabolic pathways. Among these, there was an accumulation of (R)−4'-phosphopantothenoyl-L-cysteine, a key intermediate in coenzyme A biosynthesis, and (-)-jasmonoyl-L-phenylalanine, a jasmonoyl-amino acid conjugate involved in numerous metabolic processes. Conversely, ANb application led to the down-accumulation of metabolites such as L-arginine, involved in nitric oxide biosynthesis, D-glyceraldehyde 3-phosphate, an intermediate of the Calvin-Benson cycle and L-tryptophan biosynthesis, and (-)-thujaplicatin, a compound involved in lignan biosynthesis (Fig. 3B).

Photosynthetic efficiency

Chlorophyll fluorescence parameters (Phi2, PhiNPQ and PhiNO) were analysed using ANOVA

followed by Duncan's multiple range test to assess differences among treatments (Fig. 4). Across all four measurements, the 60% N-fertilization, NI, and ANb treatments consistently exhibited the highest Phi2 values, significantly surpassing the control and 100% N-fertilization treatments in both T1 (13 DAT) and T4 (71 DAT). Specifically, at T1, Phi2 value observed in 60% N-fertilization, NI, and ANb reached 0.519 and was statistically higher by 34.1% compared to 0% N-fertilization treatment (Phi2 = 0.387) and by 26.9% compared to 100% N-fertilization treatment (Phi2 = 0.409). A similar trend was observed at T4, where the highest Phi2 value recorded in the 60% N-fertilizer, NI, and ANb (Phi2 = 0.588), was statistically higher by 73.5% compared to 0% N-fertilization (Phi2 = 0.339), by 33.9% compared to 100% N-fertilization (Phi2 = 0.439), and 43.8% compared to 100% N-fertilization and NI (Phi2 = 0.409). Notably, this treatment maintained the highest Phi2 values during heat stress conditions (coinciding with the T4 measurement), demonstrating its ability to sustain photochemical performance under adverse conditions. This combination outperformed the 100% N-fertilization treatments, suggesting that a reduced N input, combined with NI and ANb, may enhance light absorption efficiency for photosynthesis. Regarding PhiNPQ, significant differences were observed only at T2 (56 DAT), where the control (0% N-fertilization) exhibited the highest value(0.448), indicating increased non-photochemical quenching under nutrition-deficit conditions. PhiNO showed no significant differences across any of the four measurement points.

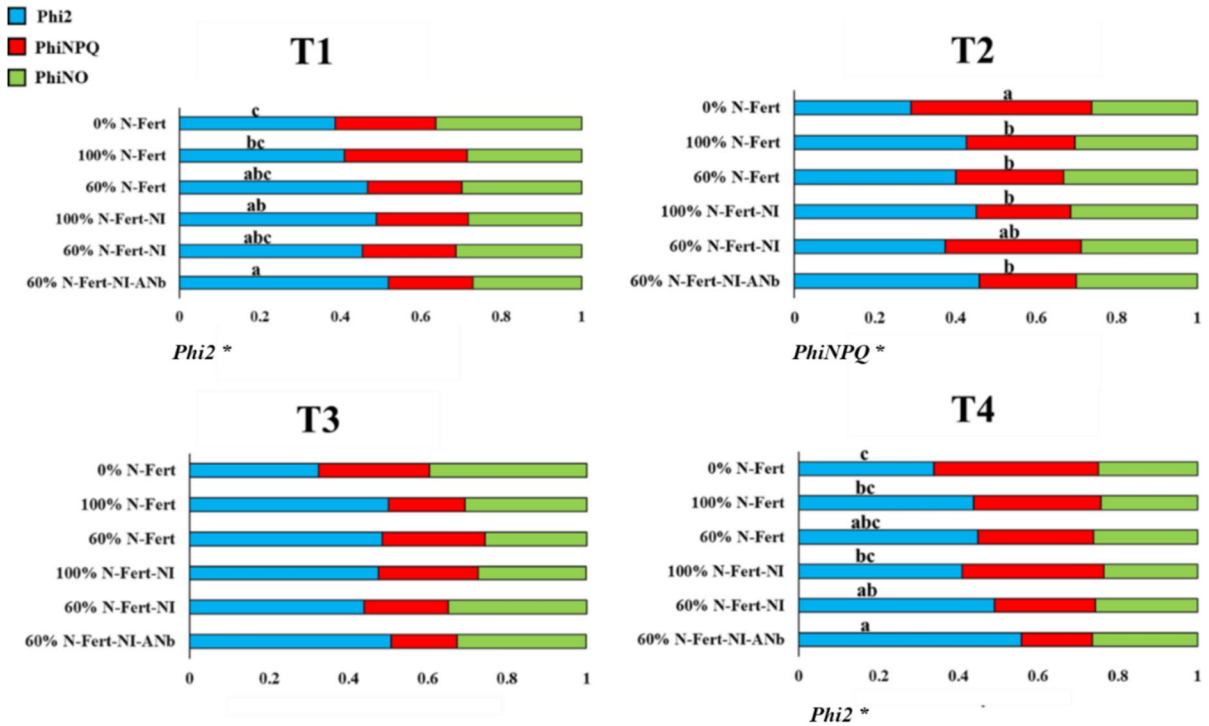

Fig. 4 Photosynthetic performance on four different times expressed as quantum yield of the photosystem II (Phi2), ratio of incoming light that is lost via non-regulated processes (PhiNO) and non-photochemical quenching (PhiNPQ) of treatments with 0% N-fertilization (treatment A), 100% N-fertilization (treatment B), 60% N-fertilization (treatment C), 100% N-fertilization and NI (treatment D), 60% N-fertilization with NI (treatment E), 60% N-fertilization with NI and ANb (treatment F). Different lowercase letters and asterisk indicate differences between treatments after one-way ANOVA with Duncan's post hoc test and significative difference (* $p < 0.05$), respectively. The four time points T1, T2, T3 and T4 corresponded to measurements taken at 13, 35, 56, and 71 DAT, respectively

Discussion

Plant performance, early nitrogen dynamics and photosynthetic traits

Our findings suggest that the impact of NI on soil nitrogen retention is influenced primarily by fertilization levels. In the 100% fertilization treatments, NI effectively inhibited ammonia oxidation, as evidenced by a 33% reduction in NO_3^- concentrations after 14 DAT. This is likely due to NI's inhibition of ammonia monooxygenases (AMO) activity in nitrifying bacteria, which prevents the conversion of NH_4^+ into NO_2^-, thereby reducing downstream NO_3^- accumulation. By day 27, NO_3^- concentrations no longer differed between treatments, yet NH_4^+ levels were twice as high in NI-treated soil. This highlights the prolonged role in maintaining ammonium availability, emphasizing its effectiveness beyond four weeks post-transplantation. These results align with previous studies showing that 3,4-DMPP significantly inhibits nitrification and sustains NH_4^+ availability in soils during short cultivation periods with chemical fertilizer application (Qiaogang et al. 2018; Benckiser et al. 2013; Barth et al. 2008).

Although nitrogen retention varied with fertilization rates, NI remained effective even at lower nitrogen inputs. At 14 DAT, NI-treated soils exhibited a significant reduction in NO_3^- accumulation, an effect that diminished by day 27 as nitrification gradually resumed. However, NH_4^+ concentrations were significantly higher in NI-treated soils early on, and while the differences were no longer statistically significant at 27 DAT, NH_4^+ levels in NI-treated soils remained 40% higher than untreated soils and were comparable to NH_4^+ levels in the 100% N-fertilization treatment without NI. This suggests that NI can partially compensate for reduced nitrogen inputs by extending NH_4^+ bioavailability, allowing plants to sustain nitrogen uptake efficiency even under suboptimal fertilization. Notably, in the 60% N-fertilization treatments, NH_4^+ availability under NI application was comparable to the 100% N-fertilization treatment without NI at 27 DAT. This suggests a 40% nitrogen reduction can maintain nitrogen homeostasis when paired with 3,4-DMPP. Wang et al. (2022) similarly demonstrated that reducing nitrogen fertilization by 40% while applying 3,4-DMPP preserved NO_3^- and NH_4^+ balance, reducing nitrogen losses while sustaining crop nitrogen uptake.

A critical aspect of NI performance is its stability under varying temperature conditions. Some reports suggest that 3,4-DMPP efficacy declines after 2–3 weeks at temperatures above 25 °C due to increased microbial degradation or volatilization of NH_4^+ (Zerulla et al. 2001; Gilsanz et al. 2016). However, in our study, NI maintained NH_4^+ retention even after 27 days at an average temperature of 27 °C, suggesting that its inhibitory effect on nitrification remained robust despite elevated temperatures. This discrepancy could be explained by site-specific microbial community differences or soil organic matter interactions, which may modulate the persistence of 3,4-DMPP's inhibitory effects (Guan et al. 2024; Bachtsevani et al. 2021).

Although ANb did not significantly affect nitrogen transformation in the soil, it played a crucial role in mitigating NO_3^- losses through leaching 14 DAT. Specifically, in the 60% nitrogen fertilization treatment with NI and ANb, NO_3^- leaching decreased by 48% compared to 60% N fertilization with NI alone. Since ANb did not directly inhibit nitrification, its effect may stem from enhanced root nitrate uptake, reducing the amount of excess NO_3^- susceptible to leaching. This aligns with previous findings indicating that *Ascophyllum nodosum* extracts can modulate nitrate transporter expression (Łangowski et al. 2022; De Saeger et al. 2020; Jannin et al. 2013), promoting efficient NO_3^- assimilation while limiting leaching losses. Interestingly, despite ANb's role in reducing NO_3^- leaching, nitrogen concentrations in biomass and fruits did not significantly increase. This suggests that its impact may be more pronounced in root-associated nitrogen cycling rather than direct assimilation into aboveground biomass. One possibility is that ANb stimulates microbial interactions that influence rhizosphere nitrogen dynamics, such as promoting beneficial root-associated bacteria capable of assimilating NO_3^-, thereby indirectly reducing nitrogen losses (Shukla et al. 2019).

The combination of the NI and ANb exhibited a moderate influence on the photosynthetic performance of plants, as indicated by consistently higher photosystem II activity (Phi2) across all four measurements. In the early stages of growth following transplantation (T1 measurement, 13 DAT), this combined treatment led to a 34.1% increase in Phi2

compared to the control. The slight enhancement in photosynthetic performance can be attributed to the presence of ANb. Consistently with the data on biomass, yields and MDA, it can be postulated that the mitigation of nutritional stress triggered by NI may have shaded, to some extent, the effect of ANb. Nonetheless, this effect on Phi2 is supported by previous evidence regarding the up modulation in the biosynthesis of photosynthetic pigments, thereby improving light-harvesting efficiency and overall photosynthetic capacity (Xiao et al. 2022; Verma et al. 2021; Tandon and Dubey 2015). Furthermore, the combined treatment with NI and ANb demonstrated greater resilience under heat stress, as evidenced by the highest Phi2 values recorded at T4 (71 DAT), which were 73.5% higher than the control. This may suggest an enhanced ability to sustain photochemical efficiency under abiotic stress conditions. The protective effect observed under heat stress may be attributed to ANb, as previous studies have highlighted its beneficial role in maintaining the photosynthetic apparatus under high-temperature conditions (Repke et al. 2022; Carmody et al. 2020) and, in general, under abiotic stresses (Staykov et al. 2020; Santaniello et al. 2017).

Distinct metabolic profiling under co-application of NI and ANb

The metabolomics profiling performed in this study provided valuable insights into the biochemical responses of tomato plants to the application of NI and ANb under reduced nitrogen fertilization. ESL showed the most pronounced metabolic changes, while LSL and root samples exhibited relatively minor differences. This suggests that the primary metabolic effects of NI and ANb are most evident during early vegetative development, likely due to the direct influence of nitrogen availability on rapidly expanding tissues. Additionally, the lack of differences observed later may be attributed to the high temperatures that the plants endured toward the end of the experiment.

In our experiments, the application of NI significantly modulated key metabolic pathways related to nitrogen assimilation and utilization. Specifically, ESL samples showed a down accumulation of amino acid biosynthesis, particularly pathways related to glutamate, asparagine, and branched-chain amino acids. This response may be interpreted considering the altered balance between NH_4^+ and NO_3^- availability induced by NI application. As evidenced by soil nitrogen analyses, NI was effective under both 100% and 60% N-fertilization regimens in slowing nitrification and in maintaining a higher availability of NH_4^+ in the soil, which may have shifted plant nitrogen uptake preferences and, in turn, driven adjustments in nitrogen metabolic pathways. In GS-GOGAT, glutamate and asparagine are accumulated to act as key nitrogen transport molecules (Gaufichon et al. 2016; Forde and Lea 2007), and their down-accumulation could suggest a reduced reliance on nitrate-dependent nitrogen assimilation by modulating plant nitrogen uptake strategies. Moreover, NI-treated plants showed a down accumulation of phenylpropanoid and flavonoid biosynthesis pathways, mainly involved in secondary metabolism and stress responses. This finding may suggest a possible metabolic trade-off, wherein nitrogen metabolism is prioritized over carbon-based secondary metabolite production. Aligning with those results, studies have demonstrated how plants grown under nitrogen-enriched conditions tend to allocate metabolic resources toward primary growth processes rather than stress-related defence compounds (Sun et al. 2020). Additionally, suppressing flavonoid biosynthesis could imply a reduced investment in antioxidant defences by plants, assuming a crucial role in mitigating oxidative stress under nutrient imbalances.

Interestingly, including ANb in combination with NI resulted in a unique metabolic profile distinct from NI-alone treatments. Indeed, one of the most striking effects was observed by the accumulation of lipid biosynthesis pathways, particularly those associated with cuticular wax formation and membrane lipid remodelling. Specifically, the increased accumulation of 16-feruloyloxypalmitate and 16-sinapoyloxypalmitate, cuticular precursors, could be an adaptive response to enhance water retention. Modulating membrane lipid composition is a well-documented strategy in plants exposed to nutrient fluctuations and environmental stressors (Bian et al. 2023). This further supports the hypothesis that ANb contributes to enhanced abiotic stress resilience. Moreover, ANb-treated plants showed significant increases in jasmonate and alkaloid biosynthesis, suggesting a potential enhancement of plant defense mechanisms not observed in NI-alone treatments. The accumulation of (-)-jasmonoyl-L-phenylalanine suggests a role in modulating stress responses, as jasmonate conjugates

are known to be involved in plant signalling pathways related to abiotic stress resistance (Per et al. 2018).. Taken together, these results are consistent with a potential involvement of ANb in regulating nitrogen assimilation under low nitrogen conditions and with metabolic adjustments commonly associated with plant response to environmental stress. In this context, the observed patterns support the hypothesis that ANb may exert a dual role by influencing nitrogen assimilation and plant defense responses when nitrogen availability is limited.

Venn analysis revealed that plants treated with both NI and ANb shared a unique set of metabolites absent in other treatments. Coherently to pathway analysis outcomes, some metabolites were involved in cell membrane integrity, lipid signalling, and nitrogen recycling pathways, highlighting that the combined application enhances nutrient efficiency and stress resilience. For example, the accumulation of all-trans-lycopene and phosphatidylcholine derivatives suggests an improved photosynthetic performance (Sathasivam et al. 2021) and membrane stability (Yu et al. 2021), crucial for sustaining plant productivity under varying environmental conditions. The accumulation of metabolites related to photosynthesis processes, together with the consistently higher photosynthetic efficiency (Phi2) observed under the combined ANb and NI treatment, further supports the hypothesis that the combined application under low nitrogen input may enhance overall photosynthetic performance. Additionally, the observed down-accumulation of L-arginine and D-glyceraldehyde 3-phosphate in ANb-treated plants may suggest an interplay between nitrogen metabolism and carbon assimilation. Since L-arginine plays a role in nitric oxide synthesis, its reduced accumulation may indicate a shift toward alternative nitrogen utilization strategies, possibly favoring NH_4^+ over NO_3^- as the dominant nitrogen. Furthermore, the reduction of lignan biosynthesis (e.g., (-)-thujaplicatin) may be explained as ANb's capability to modulate carbon partitioning away from secondary metabolite production instead of prioritizing nitrogen assimilation and primary metabolic functions. This reallocation supports the hypothesis that ANb may be involved in potential roles related to the optimization of nitrogen metabolism and carbon–nitrogen balance in plants, processes that are commonly associated with growth regulation and stress resilience. These findings indicate that the combined use of NI and ANb may offer a synergistic strategy to improve nitrogen use efficiency and plant resilience by fine-tuning nitrogen assimilation and stress signalling pathways in an early stage of plant growth.

Low nitrogen rate and NI affected yield, nitrogen uptake by fruits, and MDA analysis

Agronomic data showed that applying the reduced nitrogen rate in combination with the NI resulted in comparable yields and nitrogen uptake to those achieved with full nitrogen fertilization. Specifically, treatments with 60% N-fertilizer combined with the NI resulted in the highest tomato yield, statistically comparable to plants receiving 100% N-fertilizer. The presence of ANb did not provide any additional benefit. This outcome aligns with the inhibitory effect of NI on soil nitrification, which prolongs NH_4^+ availability and enhances its availability for root uptake, thereby optimizing nitrogen uptake and utilization efficiencies (Martínez et al. 2017; Pasda et al. 2001). Consistent with our findings, several studies reported that reducing nitrogen fertilization in combination with 3,4-DMPP can sustain yields and fruit quality comparable to those achieved with higher fertilizer application rates (Wang et al. 2022; Nie et al. 2022). However, no yield improvement was observed when the inhibitor was applied alongside full fertilization, highlighting that the same productivity levels can be achieved with a 40% reduction in fertilizer when NI is used.

Due to the occurrence of elevated temperatures, particularly during the final stage of the experiment, the MDA assay was considered a reliable indicator of free radical-induced damage to the cell membrane and an effective tool for evaluating the ability of treatments to mitigate heat-induced damage (Liu and Huang; 2000; Suzuki and Mittler 2006). Notably, the low nitrogen + NI treatment exhibited the lowest MDA content, significantly lower than all other treatments. This suggests that NI not only supports nitrogen efficiency but also reduces oxidative stress, potentially enhancing plant resilience under heat stress conditions.

Conclusions

This study highlighted how the combined application of NI and ANb could offer a promising strategy for optimizing nitrogen use in tomato plants under limited nitrogen conditions. NI effectively reduced nitrogen losses by enhancing soil NH_4^+ retention and limiting NO_3^- leaching under optimal and reduced nitrogen supplies. Noteworthy, NI treatments contributed to improved agronomic performance, with yields comparable to full nitrogen fertilization despite using 40% less nitrogen. Regarding the cooperation of NI and ANb, photosynthetic efficiency (Phi2) was slightly improved compared to other treatments, suggesting a positive impact of ANb application on photochemical energy conversion. Furthermore, metabolomic profiling revealed distinct metabolic shifts associated with stress resilience and nutrient assimilation, further supporting the benefits of this combined treatment, especially in ESL samples. Additionally, the decreased MDA level in NI-treated plants under low nitrogen conditions, either alone or ANb applied, shows a potential role in mitigating oxidative stress. Taken together, the findings corroborate the effectiveness of NI under a low nitrogen application rate while presenting positive trends in nitrogen saving and physiological aspects given by the dual usage of NI and ANb.

Acknowledgements Gianmarco Del Vecchio was the recipient of a fellowship from the Doctoral School AgriSystem from Università Cattolica del Sacro Cuore (Piacenza, Italy). The authors thank BASF Italia and Acadian for kindly providing the NI and ANb formulated products and for technical advice. The authors also thank the "Romeo ed Enrica Invernizzi" foundation (Milan, Italy) for supporting the metabolomics facility at Università Cattolica del Sacro Cuore.

Author contributions Luigi Lucini, Andrea Fiorini: Conceptualization; Gianmarco Del Vecchio, Hajar Salehi, Federico Ardenti: Formal analysis; Gianmarco Del Vecchio, Hajar Salehi, Federico Ardenti, Alejandro Castro Cegri: Investigation; Gianmarco Del Vecchio, Hajar Salehi, Federico Ardenti, Alejandro Castro Cegri: Methodology; Gianmarco Del Vecchio: Visualization; Gianmarco Del Vecchio, Hajar Salehi, Federico Ardenti: Writing-Original Draft Preparation; Luigi Lucini: Writing – Review and Editing.

Funding Open access funding provided by Università Cattolica del Sacro Cuore within the CRUI-CARE Agreement.

Data availability The data are provided as supplementary material.

Declarations

Conflict of interest The authors declare no conflict of interest.

Open Access This article is licensed under a Creative Commons Attribution 4.0 International License, which permits use, sharing, adaptation, distribution and reproduction in any medium or format, as long as you give appropriate credit to the original author(s) and the source, provide a link to the Creative Commons licence, and indicate if changes were made. The images or other third party material in this article are included in the article's Creative Commons licence, unless indicated otherwise in a credit line to the material. If material is not included in the article's Creative Commons licence and your intended use is not permitted by statutory regulation or exceeds the permitted use, you will need to obtain permission directly from the copyright holder. To view a copy of this licence, visit http://creativecommons.org/licenses/by/4.0/.

References

Abalos D, Jeffery S, Sanz-Cobena A, Guardia G, Vallejo A (2014) Meta-analysis of the effect of urease and nitrification inhibitors on crop productivity and nitrogen use efficiency. Agric Ecosyst Environ 189:136–144. https://doi.org/10.1016/j.agee.2014.03.036

Ågren GI, Wetterstedt JÅM, Billberger MFK (2012) Nutrient limitation on terrestrial plant growth – modeling the interaction between nitrogen and phosphorus. New Phytol 194:953–960. https://doi.org/10.1111/j.1469-8137.2012.04116.x

Anas M, Liao F, Verma KK, Sarwar MA, Mahmood A, Chen Z-L, Li Q, Zeng X-P, Liu Y, Li Y-R (2020) Fate of nitrogen in agriculture and environment: agronomic, eco-physiological and molecular approaches to improve nitrogen use efficiency. Biol Res 53:47. https://doi.org/10.1186/s40659-020-00312-4

Bachtsevani E, Papazlatani CV, Rousidou C, Lampronikou E, Menkissoglu-Spiroudi U, Nicol GW, Karpouzas DG, Papadopoulou ES (2021) Effects of the nitrification inhibitor 3,4-dimethylpyrazole phosphate (DMPP) on the activity and diversity of the soil microbial community under contrasting soil pH. Biol Fertil Soils 57:1117–1135. https://doi.org/10.1007/s00374-021-01602-z

Banerjee P, Garai P, Saha NC, Saha S, Sharma P, Maiti AK (2023) A critical review on the effect of nitrate pollution in aquatic invertebrates and fish. Water Air Soil Pollut 234:333. https://doi.org/10.1007/s11270-023-06260-5

Barth G, Von Tucher S, Schmidhalter U (2008) Effectiveness of 3,4-Dimethylpyrazole Phosphate as Nitriflcation Inhibitor in Soil as Influenced by Inhibitor Concentration, Application Form, and Soil Matric Potential. Pedosphere 18:378–385. https://doi.org/10.1016/S1002-0160(08)60028-4

Beeckman F, Annetta L, Corrochano-Monsalve M, Beeckman T, Motte H (2024) Enhancing agroecosystem nitrogen management: microbial insights for improved nitrification inhibition. Trends Microbiol 32:590–601. https://doi.org/10.1016/j.tim.2023.10.009

Benckiser G, Christ E, Herbert T, Weiske A, Blome J, Hardt M (2013) The nitrification inhibitor 3,4-dimethylpyrazole-phosphat (DMPP) - quantification and effects on soil metabolism. Plant Soil 371:257–266. https://doi.org/10.1007/s11104-013-1664-6

Benjamin JJ, Lucini L, Jothiramshekar S, Parida A (2019) Metabolomic insights into the mechanisms underlying tolerance to salinity in different halophytes. Plant Physiol Biochem 135:528–545. https://doi.org/10.1016/j.plaphy.2018.11.006

Bian Y, Li Q, Zhang X, Hao T, Liu N, Yang Z, Yu J (2023) Lipid composition remodeling plays a critical role during the differential responses of leaves and roots to heat stress in bermudagrass. Environ Exp Bot 213:105423. https://doi.org/10.1016/j.envexpbot.2023.105423

Calvo P, Nelson L, Kloepper JW (2014) Agricultural uses of plant biostimulants. Plant Soil 383:3–41. https://doi.org/10.1007/s11104-014-2131-8

Carmody N, Goñi O, Łangowski Ł, O'Connell S (2020) *Ascophyllum nodosum* extract biostimulant processing and its impact on enhancing heat stress tolerance during tomato fruit set. Front Plant Sci 11:807. https://doi.org/10.3389/fpls.2020.00807

Carvajal F, Palma F, Jiménez-Muñoz R, Jamilena M, Pulido A, Garrido D (2017) Unravelling the role of abscisic acid in chilling tolerance of zucchini during postharvest cold storage. Postharvest Biol Technol 133:26–35. https://doi.org/10.1016/j.postharvbio.2017.07.004

Caspi R, Dreher K, Karp PD (2013) The challenge of constructing, classifying, and representing metabolic pathways. FEMS Microbiol Lett 345:85–93. https://doi.org/10.1111/1574-6968.12194

Craigie JS (2011) Seaweed extract stimuli in plant science and agriculture. J Appl Phycol 23:371–393. https://doi.org/10.1007/s10811-010-9560-4

De Saeger J, Van Praet S, Vereecke D, Park J, Jacques S, Han T, Depuydt S (2020) Toward the molecular understanding of the action mechanism of *Ascophyllum nodosum* extracts on plants. J Appl Phycol 32:573–597. https://doi.org/10.1007/s10811-019-01903-9

Du Jardin P (2015) Plant biostimulants: definition, concept, main categories and regulation. Sci Hortic 196:3–14. https://doi.org/10.1016/j.scienta.2015.09.021

Fageria NK, Baligar VC (2005) Enhancing nitrogen use efficiency in crop plants. In: Advances in Agronomy. Elsevier, pp 97–185. https://doi.org/10.1016/S0065-2113(05)88004-6

Forde BG, Lea PJ (2007) Glutamate in plants: metabolism, regulation, and signalling. J Exp Bot 58:2339–2358. https://doi.org/10.1093/jxb/erm121

Gaufichon L, Rothstein SJ, Suzuki A (2016) Asparagine metabolic pathways in Arabidopsis. Plant Cell Physiol 57:675–689. https://doi.org/10.1093/pcp/pcv184

Gilsanz C, Báez D, Misselbrook TH, Dhanoa MS, Cárdenas LM (2016) Development of emission factors and efficiency of two nitrification inhibitors, DCD and DMPP. Agric Ecosyst Environ 216:1–8. https://doi.org/10.1016/j.agee.2015.09.030

Goñi O, Łangowski Ł, Feeney E, Quille P, O'Connell S (2021) Reducing nitrogen input in barley crops while maintaining yields using an engineered biostimulant derived from *Ascophyllum nodosum* to enhance nitrogen use efficiency. Front Plant Sci 12:664682. https://doi.org/10.3389/fpls.2021.664682

Guan T, Lei J, Fan Q, Liu R (2024) Soil factors key to 3,4-dimethylpyrazole phosphate (DMPP) efficacy: EC and SOC dominate over biotic influences. Microorganisms 12:1787. https://doi.org/10.3390/microorganisms12091787

Hawkins C, Ginzburg D, Zhao K, Dwyer W, Xue B, Xu A, Rice S, Cole B, Paley S, Karp P, Rhee SY (2021) Plant metabolic network 15: a resource of genome-wide metabolism databases for 126 plants and algae. JIPB 63:1888–1905. https://doi.org/10.1111/jipb.13163

Heath RL, Packer L (1968) Photoperoxidation in isolated chloroplasts. Arch Biochem Biophys 125:189–198. https://doi.org/10.1016/0003-9861(68)90654-1

Howarth RW (2004) Human acceleration of the nitrogen cycle: drivers, consequences, and steps toward solutions. Water Sci Technol 49:7–13. https://doi.org/10.2166/wst.2004.0731

Jannin L, Arkoun M, Etienne P, Laîné P, Goux D, Garnica M, Fuentes M, Francisco SS, Baigorri R, Cruz F, Houdusse F, Garcia-Mina JM, Yvin JC, Ourry A (2013) *Brassica napus* growth is promoted by *Ascophyllum nodosum* (L.) Le Jol. seaweed extract: microarray analysis and physiological characterization of N, C, and S metabolisms. J Plant Growth Regul 32:31–52. https://doi.org/10.1007/s00344-012-9273-9

Kramer DM, Johnson G, Kiirats O, Edwards GE (2004) New fluorescence parameters for the determination of Q_A redox state and excitation energy fluxes. Photosynth Res 79:209–218. https://doi.org/10.1023/B:PRES.0000015391.99477.0d

Kumar G, Nanda S, Singh SK, Kumar S, Singh D, Singh BN, Mukherjee A (2024) Seaweed extracts: enhancing plant resilience to biotic and abiotic stresses. Front Mar Sci 11:1457500. https://doi.org/10.3389/fmars.2024.1457500

Łangowski Ł, Goñi O, Ikuyinminu E, Feeney E, O'Connell S (2022) Investigation of the direct effect of a precision *Ascophyllum nodosum* biostimulant on nitrogen use efficiency in wheat seedlings. Plant Physiol Biochem 179:44–57. https://doi.org/10.1016/j.plaphy.2022.03.006

Lassaletta L, Billen G, Grizzetti B, Anglade J, Garnier J (2014) 50 year trends in nitrogen use efficiency of world cropping systems: the relationship between yield and nitrogen input to cropland. Environ Res Lett 9:105011. https://doi.org/10.1088/1748-9326/9/10/105011

Li H, Liang X, Chen Y, Lian Y, Tian G, Ni W (2008) Effect of nitrification inhibitor DMPP on nitrogen leaching, nitrifying organisms, and enzyme activities in a rice-oilseed rape cropping system. J Environ Sci 20:149–155. https://doi.org/10.1016/S1001-0742(08)60023-6

Li J, Van Gerrewey T, Geelen D (2022) A meta-analysis of biostimulant yield effectiveness in field trials. Front Plant Sci 13:836702. https://doi.org/10.3389/fpls.2022.836702

Liu X, Huang B (2000) Heat stress injury in relation to membrane lipid peroxidation in creeping bentgrass. Crop Sci 40:503–510. https://doi.org/10.2135/cropsci2000.402503x

Mahmud K, Panday D, Mergoum A, Missaoui A (2021) Nitrogen losses and potential mitigation strategies for a sustainable agroecosystem. Sustainability 13:2400. https://doi.org/10.3390/su13042400

Martínez F, Palencia P, Alonso D, Oliveira JA (2017) Advances in the study of nitrification inhibitor DMPP in strawberry. Sci Hortic 226:191–200. https://doi.org/10.1016/j.scienta.2017.07.046

Martínez-Alcántara B, Quiñones A, Polo C, Primo-Millo E, Legaz F (2013) Use of nitrification inhibitor DMPP to improve nitrogen uptake efficiency in citrus trees. J Agric Sci 5:1. https://doi.org/10.5539/jas.v5n2p1

Menéndez S, Barrena I, Setien I, González-Murua C, Estavillo JM (2012) Efficiency of nitrification inhibitor DMPP to reduce nitrous oxide emissions under different temperature and moisture conditions. Soil Biol Biochem 53:82–89. https://doi.org/10.1016/j.soilbio.2012.04.026

Motavalli PP, Goyne KW, Udawatta RP (2008) Environmental impacts of enhanced-efficiency nitrogen fertilizers. Crop Manag 7:1–15. https://doi.org/10.1094/CM-2008-0730-02-RV

Nie K, Bai Q, Chen C, Zhang M, Li Y (2022) DMPP and polymer-coated urea promoted growth and increased yield of greenhouse tomatoes. Horticulturae 8:472. https://doi.org/10.3390/horticulturae8060472

Pasda G, Hähndel R, Zerulla W (2001) Effect of fertilizers with the new nitrification inhibitor DMPP (3,4-dimethylpyrazole phosphate) on yield and quality of agricultural and horticultural crops. Biol Fertil Soils 34:85–97. https://doi.org/10.1007/s003740100381

Per TS, Khan MIR, Anjum NA, Masood A, Hussain SJ, Khan NA (2018) Jasmonates in plants under abiotic stresses: crosstalk with other phytohormones matters. Environ Exp Bot 145:104–120. https://doi.org/10.1016/j.envexpbot.2017.11.004

Qiao C, Liu L, Hu S, Compton JE, Greaver TL, Li Q (2015) How inhibiting nitrification affects nitrogen cycle and reduces environmental impacts of anthropogenic nitrogen input. Glob Change Biol 21:1249–1257. https://doi.org/10.1111/gcb.12802

Qiaogang Y, Junwei M, Wanchun S, Ping Z, Hui L, Changhuan F, Jianrong F (2018) Evaluations of the DMPP on organic and inorganic nitrogen mineralization and plant heavy metals absorption. Geoderma 312:45–51. https://doi.org/10.1016/j.geoderma.2017.10.007

Repke RA, Silva DMR, Dos Santos JCC, De Almeida Silva M (2022) Increased soybean tolerance to high-temperature through biostimulant based on *Ascophyllum nodosum* (L.) seaweed extract. J Appl Phycol 34:3205–3218. https://doi.org/10.1007/s10811-022-02821-z

Salehi H, Chehregani Rad A, Miras-Moreno B, Lucini L (2023) The inclusion of engineered ZnO nanoparticles and bulk $ZnSO_4$ in the growth medium distinctively modulate the root and leaf metabolome in bean plants. Physiol Plant 175:e13952. https://doi.org/10.1111/ppl.13952

Salek RM, Steinbeck C, Viant MR, Goodacre R, Dunn WB (2013) The role of reporting standards for metabolite annotation and identification in metabolomic studies. Gigascience 2:13. https://doi.org/10.1186/2047-217X-2-13

Santaniello A, Scartazza A, Gresta F, Loreti E, Biasone A, Di Tommaso D, Piaggesi A, Perata P (2017) *Ascophyllum nodosum* seaweed extract alleviates drought stress in Arabidopsis by affecting photosynthetic performance and related gene expression. Front Plant Sci 8:1362. https://doi.org/10.3389/fpls.2017.01362

Sathasivam R, Radhakrishnan R, Kim JK, Park SU (2021) An update on biosynthesis and regulation of carotenoids in plants. S Afr J Bot 140:290–302. https://doi.org/10.1016/j.sajb.2020.05.015

Shukla PS, Mantin EG, Adil M, Bajpai S, Critchley AT, Prithiviraj B (2019) *Ascophyllum nodosum*-based biostimulants: sustainable applications in agriculture for the stimulation of plant growth, stress tolerance, and disease management. Front Plant Sci 10:655. https://doi.org/10.3389/fpls.2019.00655

Staykov NS, Angelov M, Petrov V, Minkov P, Kanojia A, Guinan KJ, Alseekh S, Fernie AR, Sujeeth N, Gechev TS (2020) An *Ascophyllum nodosum*-derived biostimulant protects model and crop plants from oxidative stress. Metabolites 11:24. https://doi.org/10.3390/metabo11010024

Stewart WM, Dibb DW, Johnston AE, Smyth TJ (2005) The contribution of commercial fertilizer nutrients to food production. Agron J 97:1–6. https://doi.org/10.2134/agronj2005.0001

Sun Y, Wang M, Mur LAJ, Shen Q, Guo S (2020) Unravelling the roles of nitrogen nutrition in plant disease defences. IJMS 21:572. https://doi.org/10.3390/ijms21020572

Suzuki N, Mittler R (2006) Reactive oxygen species and temperature stresses: a delicate balance between signaling and destruction. Physiol Plant 126:45–51. https://doi.org/10.1111/j.0031-9317.2005.00582.x

Tandon S, Dubey A (2015) Effects of Biozyme (*Ascophyllum nodosum*) biostimulant on growth and development of soybean [*Glycine max* (L.) Merill]. Commun Soil Sci Plant Anal 46:845–858. https://doi.org/10.1080/00103624.2015.1011749

Verma N, Sehrawat KD, Mundlia P, Sehrawat AR, Choudhary R, Rajput VD, Minkina T, Van Hullebusch ED, Siddiqui MH, Alamri S (2021) Potential use of *Ascophyllum nodosum* as a biostimulant for improving the growth performance of *Vigna aconitifolia* (Jacq.) Marechal. Plants 10:2361. https://doi.org/10.3390/plants10112361

Vilas MP, Verburg K, Thorburn PJ, Probert ME, Bonnett GD (2019) A framework for analysing nitrification inhibition: A case study on 3,4-dimethylpyrazole phosphate (DMPP). Science of The Total Environment 672:846–854. https://doi.org/10.1016/j.scitotenv.2019.03.462

Wang F, Ge S, Lyu M, Liu J, Li M, Jiang Yu, Xu X, Xing Y, Cao H, Zhu Z, Yuanmao J (2022) DMPP reduces nitrogen fertilizer application rate, improves fruit quality, and reduces environmental cost of intensive apple production in China. Sci Total Environ 802:149813. https://doi.org/10.1016/j.scitotenv.2021.149813

Ward M, Jones R, Brender J, De Kok T, Weyer P, Nolan B, Villanueva C, Van Breda S (2018) Drinking water nitrate and human health: an updated review. IJERPH 15:1557. https://doi.org/10.3390/ijerph15071557

Xiao F, Li D, Zhang L, Du Y, Xue Y, Cui L, Gong P, Song Y, Zhang K, Zhang Y, Li Y, Zhang J, Cui Y (2022) Effect of urease inhibitors and nitrification inhibitors combined with seaweed extracts on urea nitrogen regulation and application. Agronomy 12:2504. https://doi.org/10.3390/agronomy12102504

Yu L, Zhou C, Fan J, Shanklin J, Xu C (2021) Mechanisms and functions of membrane lipid remodeling in plants. Plant J 107:37–53. https://doi.org/10.1111/tpj.15273

Zerulla W, Barth T, Dressel J, Erhardt K, Horchler Von Locquenghien K, Pasda G, Rädle M, Wissemeier A (2001) 3,4-dimethylpyrazole phosphate (DMPP) - a new nitrification inhibitor for agriculture and horticulture. Biol Fertil Soils 34:79–84. https://doi.org/10.1007/s003740100380

Publisher's Note Springer Nature remains neutral with regard to jurisdictional claims in published maps and institutional affiliations.